Design of Triple-Band MIMO Antenna with One Band-Notched Characteristic

Amit Kumar[1, 2], Abdul Q. Ansari[1], Binod K. Kanaujia[3],
Jugul Kishor[4, *], and Nidhi Tewari[5]

Abstract—A microstrip-fed two-port multiple-input-multiple-output (MIMO) antenna has been designed for triple-band applications covering the entire ultra-wideband (UWB) with one band-notched characteristic. A defected ground structure (DGS) has been used to obtain a wideband resonance. A crescent ring has been etched on each of the two circular patch antennas to produce a band-notch characteristic centered at 5 GHz, ranging from 3.96 to 6.2 GHz. These introduce notches at 5.2/5.8 WLAN, 5.5 WiMAX, LMI C-Band and also reject the large capacity microwave relay trunk network, ranging from 4.40 to 4.99 GHz, such as in the Indian national satellite (INSAT) system operating between 4.5 and 4.8 GHz, thus making our MIMO antenna immune to many unlicensed bands. The proposed MIMO antenna elements have been isolated by more than 16 dB throughout the operating band using a modified inter-digital capacitor (MIDC) placed between the circular patch antennas. The MIDC also helps in achieving a center-band, ranging from 6.2 to 8.93 GHz and is useful in IEEE INSAT/Super Extended C-band. The lower-band ranges from 3.08 to 3.96 GHz and covers 3.5 GHz WiMAX while the upper-band, ranging from 10 to 16 GHz, is useful for X-band and Ku-band applications. Finally, the MIMO antenna has been fabricated on an FR-4 substrate of dimensions $50 \times 30 \times 1.6$ mm^3 with a compact antenna area of $0.158\lambda_0^2$. All results along with the diversity performance have been experimentally verified.

1. INTRODUCTION

In 2002, the Federal Communications Commission (FCC) released an unlicensed ultra-wideband (UWB) spectrum, ranging from 3.1 to 10.6 GHz [1], for future communication. Since then, there has been an increase in demand of designing UWB systems for handling high data rates in the presence of wireless communications standards, which causes electromagnetic (EM) interference [2] such as 5.2/5.8 GHz-wireless local area network (WLAN) system, 5.5 GHz-worldwide interoperability for microwave access (WiMAX) system, INSAT operating between 4.5 and 4.8 GHz and many more. So, the design of UWB MIMO antennas with band-notches becomes very popular. The demand for high data rates can be achieved by MIMO systems without sacrificing additional spectrum and transmitted power in a rich scattering environment [3]. Designing compact MIMO antennas with reduced mutual coupling having less polarization mismatch, and immune to noisy and fading channels is a big challenge. Several mutual coupling reduction techniques were introduced in previous researches such as a planar Electromagnetic Gap (EBG), and multilayer dielectric substrate was used to improve isolation by 10–15 dB [4]. Similarly miniaturized Double-Layer EBG structures were used to increase isolation between UWB monopoles [5].

* Corresponding author: Jugul Kishor (er.jugulkishor@gmail.com).
[1] Department of Electrical Engineering, FET, Jamia Millia Islamia, New Delhi, India. [2] Darbhanga College of Engineering, Darbhanga, Bihar, India. [3] School of Computational and Integrative Sciences, Jawahar Lal Nehru University, New Delhi, India. [4] Department of Electronics & Communication Engineering, I.T.S Engineering College, UP, India. [5] Department of Electronics & Communication Engineering, SECE, Galgotias University, UP, India.

Split-Ring Resonator (SRRs) being modified and used as an isolation structure like Folded Split-Ring Resonators (FSRRs) used in [6] resulted in 30 dB isolation while Slotted-Complementary Split-Ring Resonators used in [7] resulted in 10 dB reduction in mutual coupling effect. A simple slot in the common ground plane results in an isolation of 40 dB among antenna elements separated by a mere distance of $0.33\lambda_0$ [8]. A wideband neturalization line resulted in an isolation of 22 dB for the UWB MIMO antenna operating from 3.1 to 5 GHz [9]. Some more techniques of mutual coupling reduction were listed in [10]. The focus has been made on designing a UWB MIMO antenna with band-notches to avoid EM interference from unwanted frequency spectrum considering a particular host system application. Recently, many UWB MIMO antennas with one or more band-notched characteristics have been designed as described below. In [11], a UWB MIMO antenna with a band-notch ranging from 5 to 6 GHz having minimum 15 dB isolation was implemented. A dual-band-notched UWB MIMO antenna having a rejection in WiMAX and International Telecommunication Union (ITU) band was proposed in [12]. Multiple band-notch bands were implemented using an underground filter in a CPW-fed circular-disk UWB antenna [13]. Another UWB antenna with notches at 5.5/5.8 WLAN and 3.5/5.5 GHz WiMAX was introduced in [14]. A triple-band-notched UWB antenna having notches around WiMAX and WLAN was created using concentric split-ring slots structure [15]. Koch structure and T-shaped stub were used [16] to create a band-notch around PCS, WiMAX, and WLAN. A dual band-notched characteristic compact UWB MIMO antenna, which introduced notches at WLAN and IEEE INSAT/Super-Extended C-band, was designed with inverted L-shaped slits having a minimum isolation of 22 dB [17]. Other dual band-notched UWB MIMO antennas are: a novel filtenna having notched bands of 3.35–3.55 GHz and 5.65–5.95 GHz with a minimum isolation of 20 dB [18], a compact co-planar waveguide (CPW)-fed circular patch MIMO antenna having etched split ring resonator (SRR) slot in the radiator, which results in one band-notch centered at 7.6 GHz and a band-notch at 5G WLAN achieved by the collaboration of the arc-shaped strips with an isolation of 15 dB [19], and in another case, the radiation patch was connected with the strip placed beneath the patch through a via to achieve band-notch at WiMAX (3.4–3.7 GHz) and WLAN (5.15–5.35 and 5.725–5.825 GHz) [20]. Many single band-notched UWB MIMO antennas have been designed around 5G WLAN: a printed folded monopole antenna with an open stub inserted in the antenna to reject the 5G WLAN [21], CPW-fed staircase-shaped radiators with etched SRR results in band-notch [22], circular CPW feeding structures loaded by arc-shaped slot resonators to reject the undesired sub-band, which was assigned for IEEE 802.11a and HIPERLAN/2 [23], microstrip-fed antenna elements with L-shaped slits etched on the ground plane resulting in the band-notched band at 5.5 GHz [24], two squares monopole-antenna elements with two strips on the ground plane creating a band-notched frequency band [25], a G-shaped structure on the square antenna element formed to achieve the band-reject from 4.4–6.2 GHz [26], and two folded slots inserted in heptagonal radiators to achieve band-notch at WLAN [27]. Two more UWB MIMO antennas, having band-notch around C-band, were implemented like a quad-element with band-notched from 4.0–5.2 GHz with reduced mutual coupling due to electromagnetic band-gap (EBG) structures had been implemented [28]. In the second case, MIMO had an L-shaped stub, extruded in the ground plane to introduce band-notched function C-band (3.62–4.77 GHz) [29]. A few single element antennas with band-notched characteristics are: a quad band-notched (3.3–3.7 GHz, 4.5–4.8 GHz, 5.15–5.35 GHz, and 5.725–5.825 GHz bands) UWB antenna created using four different ring resonators on multilayered planes [2], and in another MIMO antenna, the band-reject (6.70–7.1 GHz) was achieved by attaching a strip to the hollow center of a wing-shaped monopole [30]. A comparison is provided below in Table 1 along with the proposed MIMO antenna to have a better overview of the ongoing research.

In this paper, a triple-band MIMO antenna is proposed for UWB applications along with one band-notched characteristic centered at 5 GHz to block the WLAN frequency. We are focused on blocking 5 GHz WLAN/WiMAX as well as some part of C-band which covers the high traffic of microwave relay trunk network ranging from 4.10 to 4.99 GHz. The proposed triple-band MIMO antenna covers 3.08–3.96, 6.2–8.93 GHz & 10–16 GHz bands, respectively, thus covering the entire UWB, along with one band-notched characteristic from 3.96–6.2 GHz. A defected ground structure (DGS) has been used to obtain a wideband resonance. A crescent ring has been etched on each of the two circular patch antennas to produce a band-notch characteristic which introduces notches at 5.2/5.8 WLAN, 5.5 WiMAX and LMI C-band. In addition, the proposed antenna also rejects the large capacity microwave relay trunk network, ranging from 4.40 to 4.99 GHz, such as in the Indian national satellite (INSAT) system operating between

4.5 and 4.8 GHz, thus making our MIMO antenna immune to many unlicensed bands. The isolation structure-MIDC has been placed between the circular patch antennas to improve the isolation from 10 to 25 dB in the lower band along with a minimum measured isolation, better than 16 dB between the ports throughout the operating bands. The band-notch has already resulted in dual-band operation, while the third-band is achieved due to better impedance matching after the introduction of isolation structure MIDC, which also ensure that our proposed antenna does not interfere with X-band ranging from 8.93 to 10 GHz. The second band (6.2–8.9 GHz) is useful in IEEE INSAT/Super Extended C-band applications. The upper-band, ranging from 10 to 16 GHz, is useful for X-band and Ku-band applications. Another added advantage of our proposed antenna, as shown in Table 1, is that it has better isolation and compactness than the majority of the MIMO antennas designed recently.

Table 1. Comparisons with the existing UWB MIMO band-notched antennas.

Ref.	Antenna Elements	Band-Notched Frequencies (GHz)	Minimum Isolation (dB)	Ant. Area (λ_0^2)	Substrate
[17]	2	5.1–5.8, 6.7–7.1	22	0.061	FR-4
[18]	2	3.35–3.55, 5.65–5.95	20	0.441	$\varepsilon_r = 2.65$
[19]	2	centered at 5.6 & 7.6	15	0.202	FR-4
[20]	2	3.4–3.7, 5.15–5.825	15	0.127	FR-4
[21]	2	5.15–5.85	17.2	0.027	FR-4
[22]	2	5.1–6	15	0.160	FR-4
[23]	2	4.75–6.12	15	0.211	Rogers 6035
[24]	2	5.03–5.97	15	0.156	FR-4
[25]	2	5.15–5.85	15	0.081	Rogers 4350
[26]	2	4.4–6.2	15	0.222	FR-4
[27]	2	centered at 5	20	0.175	PET Film
[28]	4	4.0–5.2	17.5	0.360	FR-4
[29]	2	3.62–4.77	20	0.065	FR-4
Prop.	2	3.96–6.2	16	0.158	FR-4

2. ANTENNA DESIGN AND THEORY

The design process of the triple-band MIMO antenna has been divided into two sections: Section I deals with the design and evolution of the single antenna element with the desired band-notch characteristics around 3.96–6.2 GHz, and Section 2 describes how this single element has been integrated into a two-port MIMO antenna and also discusses the introduced MIDC isolation structure which also helps in improving the impedance matching and achieving the center-band covering 6.2–8.93 GHz, and thus, helps in realizing a triple-band MIMO antenna covering UWB with one band-notched characteristic. The proposed MIMO antenna has been fabricated on an FR-4 ($\varepsilon_r = 4.4$, $\tan \delta = 0.025$) substrate of dimensions $50 \times 30 \times 1.6 \, \text{mm}^3$.

2.1. Section I

First, we will go through the design process of a single element of the proposed MIMO antenna. The design evolution has gone through three steps as shown in Figure 1. In CASE I, a simple microstrip-fed monopole circular patch antenna, with a rectangular ground plane, has been considered, resulting in a band operation ranging from 6.76 to 9.72 GHz and having a reflection coefficient of -9 dB centered around 5 GHz. Our objective of achieving band-notch centered around 5 GHz WLAN has been achieved with the introduction of an etched crescent ring-shaped structure on the circular radiating patch as
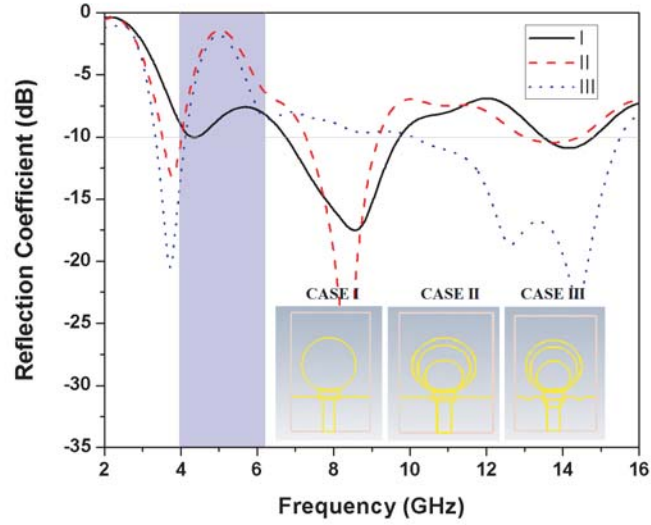
Figure 1. Evolution of the single element of MIMO antenna and its reflection coefficient.

shown in CASE II of Figure 1. The reflection coefficient has been increased to -1 dB around 5 GHz (3.96–6.2 GHz), and thus, it reduces the antenna efficiency way below, such that the proposed antenna gets isolated from 5.2/5.8 WLAN, 5.5 WiMAX, LMI C-band and also rejects the large capacity microwave relay trunk network ranging from 4.40 to 4.99 GHz as in the Indian national satellite (INSAT) system operating from 4.5 to 4.8 GHz, thus making our antenna immune to many unlicensed bands.

With the introduction of three semicircles in the ground plane, there is an increased bandwidth of the antenna such that it becomes a UWB antenna, as shown in CASE III of Figure 1. Out of the three semicircles, two are of the same radius, while the middle one has a larger radius. The entire dimension has been discussed precisely in the next section. There is an impedance matching problem in the middle of the operating range of the UBW as shown in CASE III, which has been optimized in MIMO designing, discussed in the next section. The band-notch has been widened as compared to the previous work shown in [28] by reducing the area of the ground plane, and hence, reduced the antenna area required for the same purpose. Also, in spite of covering the entire UWB as done in [28], the semicircle radius has been reduced considerably to avoid some part of the X-band in comparison to the MIMO antenna defined in [28].

2.2. Section II

The final design of CASE III in Section-1 has been taken to design a two-port MIMO antenna as shown in Figure 2. An isolation structure, based on the concept of the interdigital capacitor (IDC) [31], has been introduced as shown in Figure 2(b), which is further improved with modified IDC to achieve better impedance matching as claimed in the S-parameters analysis, as shown in Figure 4.
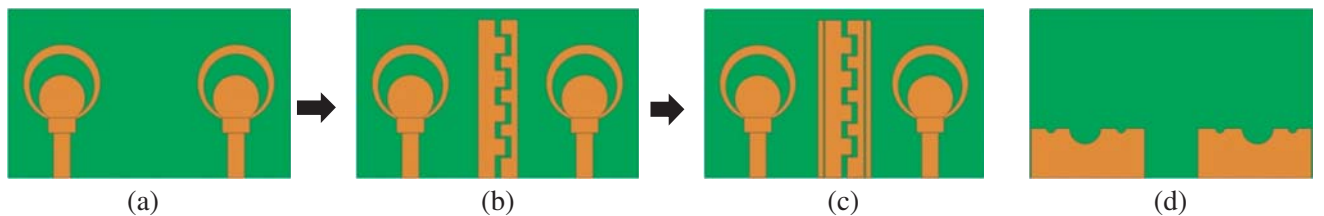

Figure 2. Design steps of two-port MIMO antenna. (a) Circular monopole crescent ring. (b) Circular monopole with IDC. (c) Circular monopole with MIDC. (d) Back view with DGS.
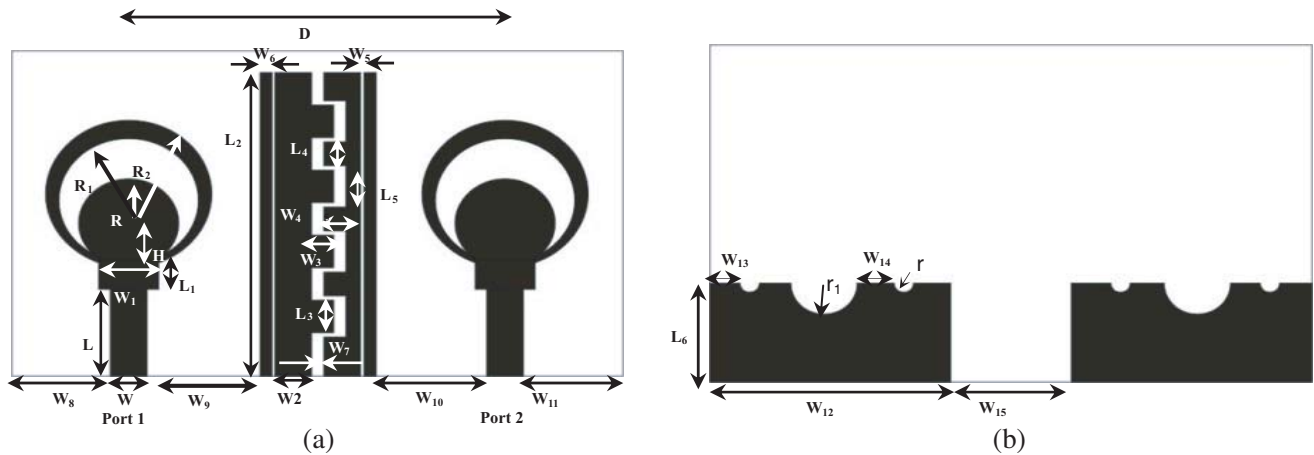
Figure 3. Geometry of the proposed MIMO antenna. The dimensions of the MIDC are $W_2 = 3$, $L_2 = 28$, $W_3 = 1.8$, $L_3 = 3$, $W_4 = 1.8$, $L_4 = 2.2$, $L_5 = 3.75$, $W_5 = 0.225$, $W_6 = 1$, $W_7 = 0.95$. The other dimensions of the antenna are $W_8 = 8.35$, $W_9 = 8.95$, $W_{10} = 8.85$, $W_{11} = 8.45$, $W_{13} = 2.5$ and $W_{14} = 3.1$ (All dimensions are in mm). (a) Front view. (b) Back view.
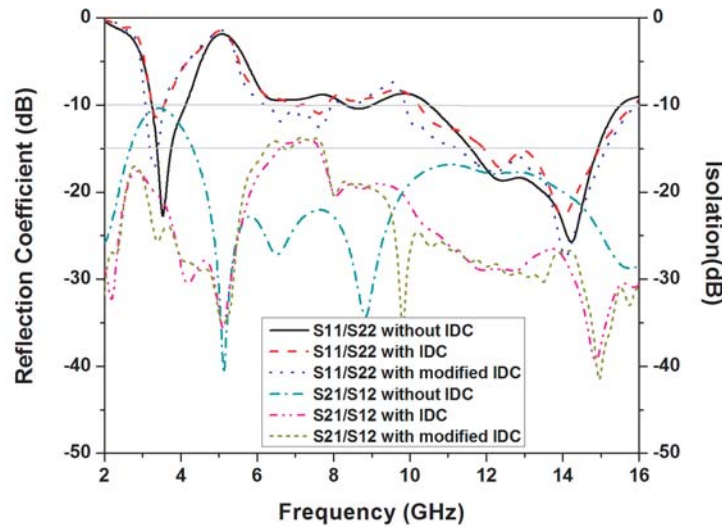

Figure 4. Simulated S-parameters: with and without IDC & MIDC.

The complete layout of the proposed triple-band MIMO antenna is given in Figure 3. The two circular monopole antenna elements are placed parallel to each other, unlike [28], to reduce the antenna area with a center-to-center distance of $D = 30.2$ mm ($0.31\lambda_0$), but the isolation is only 10 dB, as shown in Figure 4. The circular monopole antenna consists of three circles of radii $R = 4.1$ mm, $R_1 = 5.7$ mm and $R_2 = 6.8$ mm, where the center is counted above the signal strip of $W_1 = 4.9$ mm and $L_1 = 2.7$ mm at height $H = 4$ mm. The dimensions of the transmission strip are $W = 3$ mm and $L = 8$ mm. The distance between the DGSs has an effect on impedance matching, so the closer the structures are moved, the better impedance matching will be achieved. After optimization, good impedance matching is achieved at a gap width of 10 mm (W_{15}). The dimension of the rectangular ground structure is $W_{12} = 20$ mm and $L_6 = 8.8$ mm as shown in Figure 3(b) which is reduced from the previous case [28] of 28.8×8.8 mm^2. The three semicircles of radii $r = 0.8$ mm (two are of the same radius) and $r_1 = 2.5$ mm are etched on the rectangular ground. The radius of the semicircle is optimized so that it avoids some part of

the X-band frequency ranging from 8.93 to 10 GHz, which can be clearly observed in the S-parameters analysis shown in Figure 4.

The number of fingers (= 9) in IDC, as well as the length L_2, is optimized using the concept mentioned in [31] to create a band-stop filter centered around 3.5 GHz. The isolation structure with IDC helps in improving the isolation from 10 dB to 20 dB in the lower band, which further increases to 25 dB in the case of MIDC. Thus, we are successful in achieving a better isolation of 25 dB with MIDC in the lower-band than 17.5 dB [28] in the previous one. We are also able to achieve a compact area of $0.158\lambda_0^2$ as compared to $0.18\lambda_0^2$ [28] in the earlier case after considering only two antenna elements and to avoid some part of the X-band as stated earlier; however, our isolation is slightly disturbed in the center-band, where we are able to achieve a measured isolation of 16 dB.

3. RESULTS AND DISCUSSION

The proposed MIMO antenna has been fabricated as shown in Figure 5. The measured S-parameters analyzed in Figure 6 experimentally verified the resemblance with the simulated results.

The measured isolation is more than 16 dB throughout the operating bands. The above results show
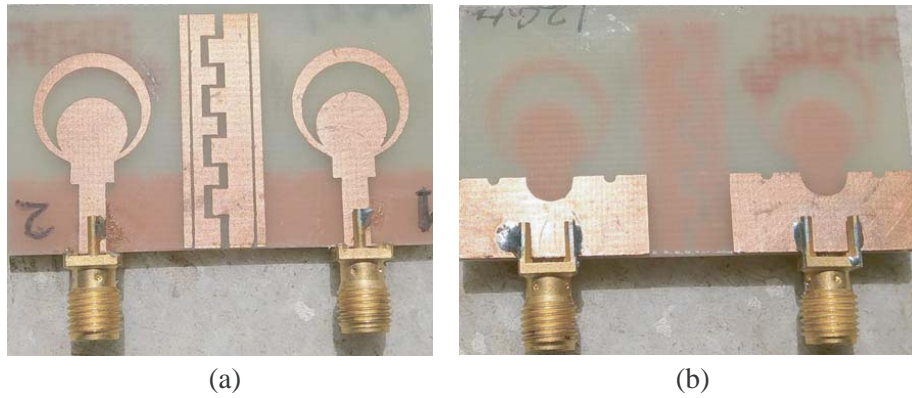

(a)   (b)

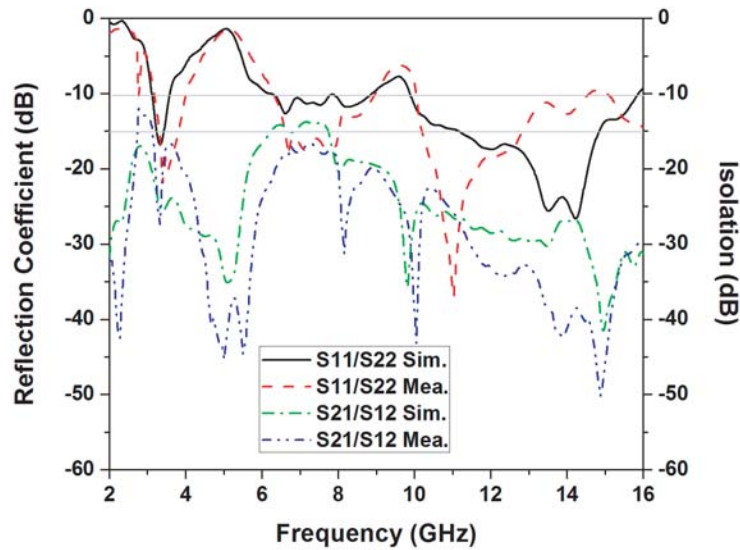**Figure 5.** Fabricated MIMO antenna. (a) Front View. (b) Back View.

Figure 6. Simulated and measured S-parameters with MIDC.

that our proposed antenna is a triple-band antenna: 3.08–3.96, 6.2–8.93 GHz & 10–16 GHz, covering the entire UWB, along with a band-notched characteristic from 3.96 to 6.2 GHz. The range from 8.93 to 10 GHz cannot be claimed as band-notch, but it will restrict some part of the X-band.

The gain and radiation efficiency are shown in Figure 7, which clearly shows the immediate drop in gain around the band-notch, going as low as 2 dBi from 5 dBi, so the radiation efficiency has been lowered to 20% from 80% which is centered at 5 GHz. Our antenna performance is also hindered around 8.93–10 GHz where the reflection coefficient goes as high as −5 dB, and thus, restricting it from some part of the X-band.

The surface current distribution and E-field distribution at 3.5 GHz have been represented in Figures 8(a) & (b), respectively, after exciting port-1 and terminating port-2 with 50 Ω load. Clearly,

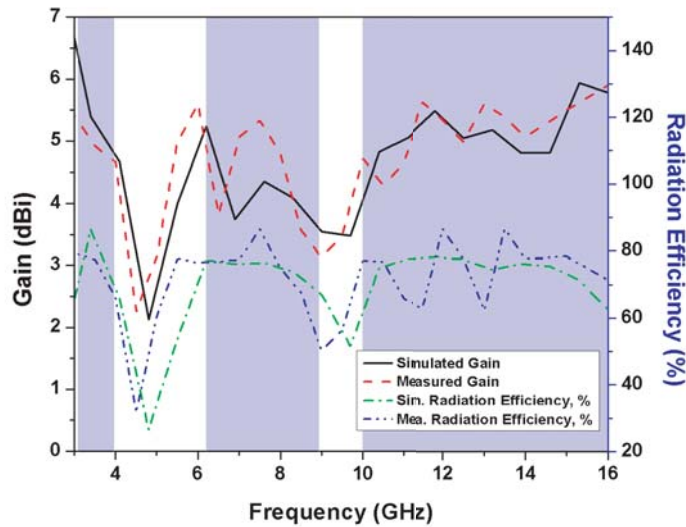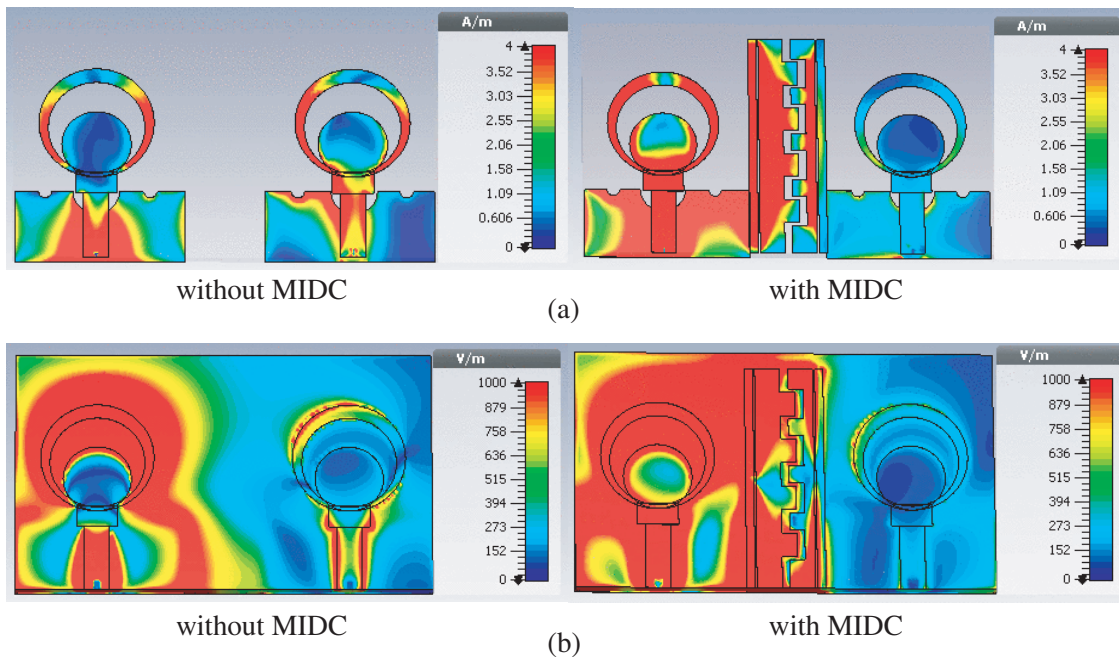**Figure 7.** Gain and efficiency of the proposed antenna.

Figure 8. (a) Surface current distribution and (b) E-field distribution at 3.5 GHz.

in Figure 8(a), we can see how surface wave propagation from the first antenna to the second has been restricted by the introduction of MIDC as the current density has been significantly reduced on the terminated second antenna compared to the MIMO antenna without MIDC structure. Similarly, in Figure 8(b), the electric field distribution inside the substrate has also been significantly reduced with MIDC structure, thus strengthening the isolation behavior of the MIDC by restricting the space wave propagation from the first antenna to the second and vice-versa.

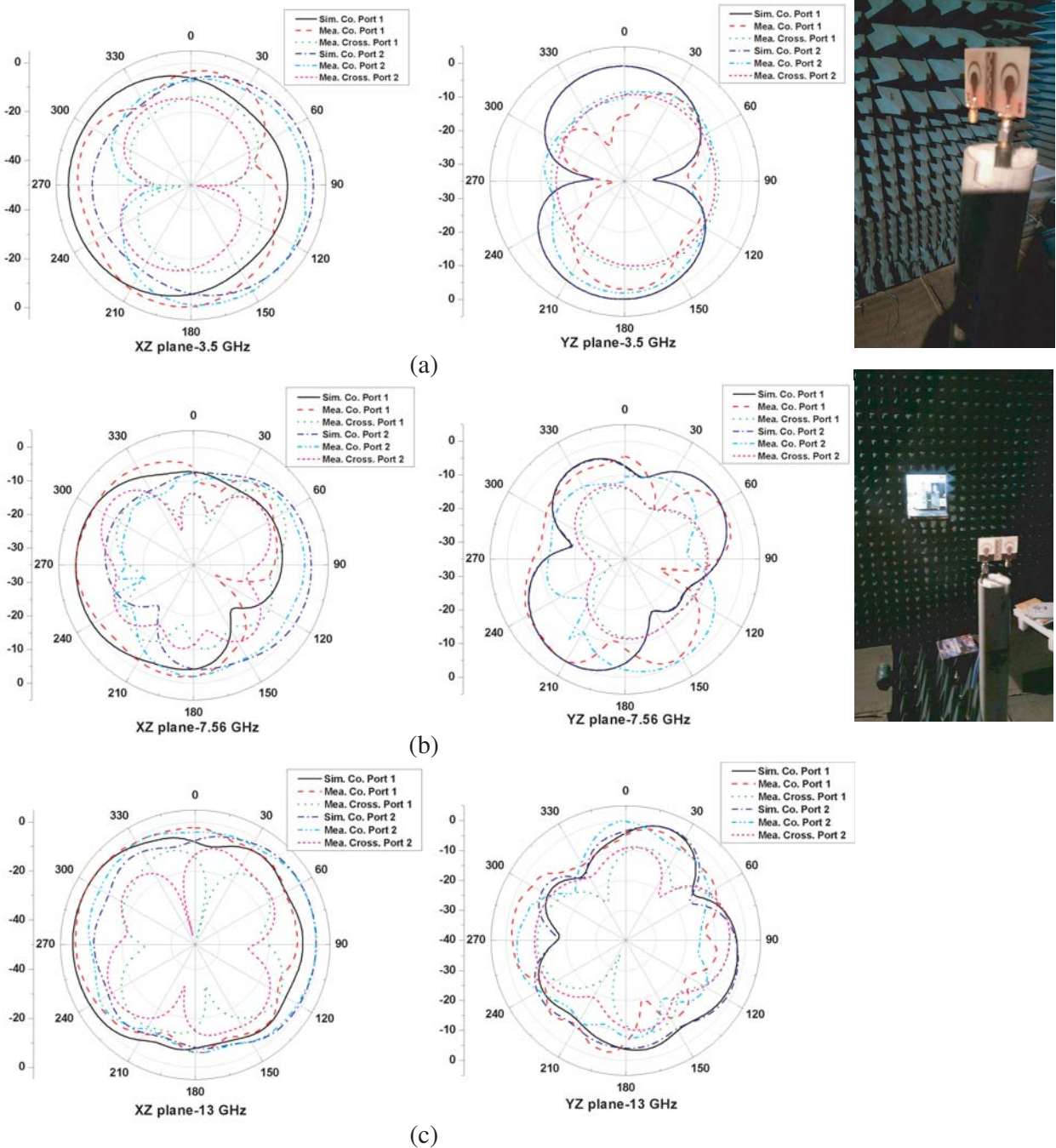The normalized radiation patterns are shown in Figure 9. E-plane (XZ plane) and H-plane (YZ

Figure 9. E-plane (XZ plane) and H-plane (YZ plane) radiation patterns at three resonant frequencies, (a) 3.5 GHz, (b) 7.56 GHz and (c) 13 GHz.

plane) have been represented at each of the three resonant bands after exciting one port and terminating the other. The purpose of the MIMO antenna is to achieve an omnidirectional pattern with the help of its antenna elements, and thus, prevent signal dropout irrespective of the direction of signal's arrival. We can see the E-plane (XZ plane) in Figure 9, which shows that the omnidirectional pattern has been maintained at all the three resonant frequencies. Cross- and co-polarizations show their isolated behavior in E-plane except for fewer points.

4. DIVERSITY PERFORMANCE

This section will discuss the diversity performance of our MIMO antenna which is necessary to figure out the isolated behavior of each of the individual antenna elements present in the MIMO system.

4.1. ECC (Envelope Correlation Coefficient)

ECC defines the correlation coefficient between the signals received from different antenna elements which increase the throughput of the signal. The criterion for MIMO antenna is ECC < 0.05 [3]. ECC of a general two-antenna system can be determined by the following formula [3]:

$$\rho e(i, j, N) = \frac{\left| \sum_{n=1}^{N} S_{i,n}^* S_{n,j} \right|^2}{\Pi_{k=(i,j)} \left[1 - \sum_{n=1}^{N} S_{i,n}^* S_{n,k} \right]} \tag{1}$$

where i and j are the antenna elements, and N is the total number of antennas.

The equation of ECC for a two-port MIMO antenna can be written as below:

$$\rho e(1, 2, 2) = \frac{|S_{11}^* S_{12} + S_{12}^* S_{22}|^2}{\left(1 - \left(|S_{11}|^2 + |S_{21}|^2 \right) \right) \left(1 - \left(|S_{12}|^2 + |S_{22}|^2 \right) \right)} \tag{2}$$

The computed ECC from the given equation is shown in Figure 10 for both simulated and measured results. We can see that the ECC < 0.01 for the entire operating range.
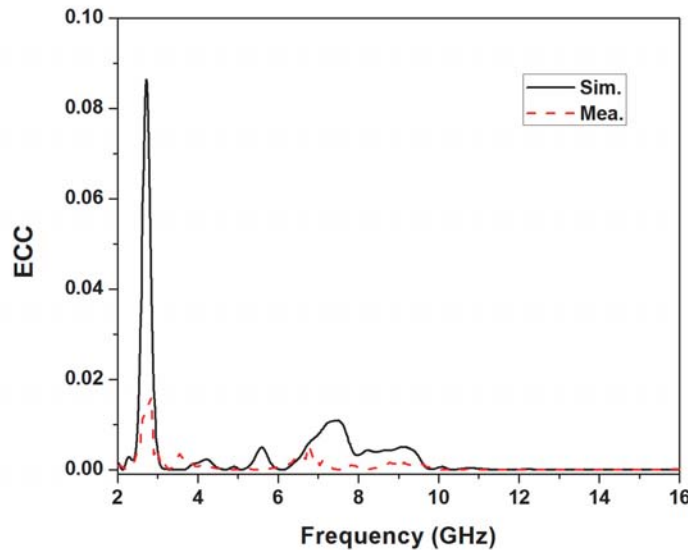
Figure 10. Computed ECC.

4.2. MEG (Mean Effective Gain)

In a fading environment, MEG is the measure of the amount of power received by the antenna elements as compared to an isotropic antenna. We can compute the MEG using the following equations [3]:

$$\text{MEG}_i = 0.5 \left[1 - \sum_{j=1}^{N} |S_{ij}|^2\right] < -3\,\text{dB} \tag{3}$$

$$\text{Also} \qquad |\text{MEG}_i - \text{MEG}_j| < 3\,\text{dB} \tag{4}$$

So, MEG_1 and MEG_2 can be written as,

$$\text{MEG}_1 = 0.5 \left[1 - |S_{11}|^2 - |S_{12}|^2\right] \tag{5}$$

$$\text{MEG}_2 = 0.5 \left[1 - |S_{21}|^2 - |S_{22}|^2\right] \tag{6}$$

As shown in Figure 11, MEG is below $-3\,\text{dBi}$, and also, the difference between the MEG_1 and MEG_2 is within the range of $\pm 3\,\text{dB}$.
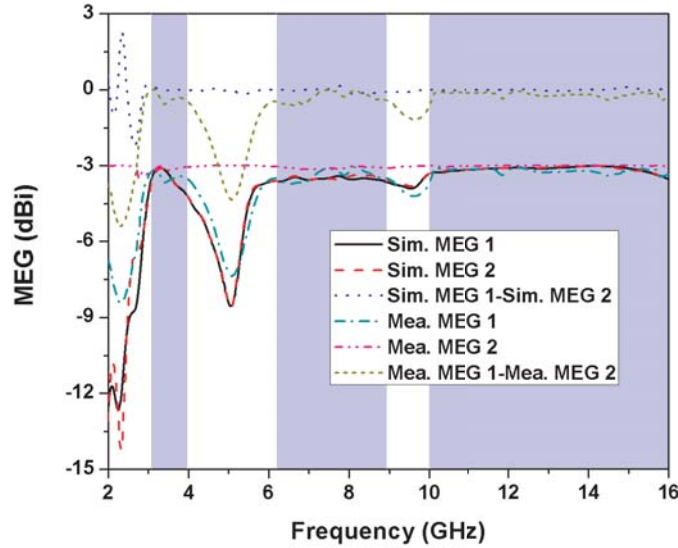

Figure 11. MEG.

4.3. CCL (Channel Capacity Loss)

CCL defines the maximum attainable limit of information transmission rate up to which the signal can be easily transferred without a significant loss which is defined to be less than $0.4\,\text{bits/s/Hz}$ [3]. It can be computed using the following equations [3]:

$$C_{loss} = -\log_2 \det\left(\alpha^R\right) \tag{7}$$

where $\alpha^R = \begin{bmatrix} \alpha_{11} & \alpha_{12} \\ \alpha_{21} & \alpha_{22} \end{bmatrix}$; where $\alpha_{ii} = 1 - (\sum_{j=1}^{N} |S_{ij}|^2)$ and $\alpha_{ij} = -(S_{ii}^* S_{ij} + S_{ji}^* S_{ij})$.

We can see that the computed CCL is below $0.4\,\text{bits/s/Hz}$ for the entire operating range as shown in Figure 12.
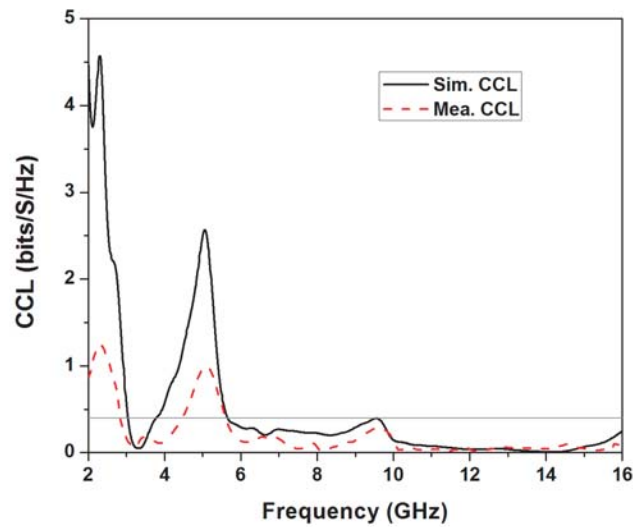
Figure 12. CCL.

4.4. TARC (Total Active Reflection Coefficient)

TARC signifies the importance of non-variance of the resonance frequency and the IBW (Impedance Bandwidth) even when the phase of the input signals, say θ, is changing with respect to the other antenna elements [3]. It can be computed using the following equations [3]:

$$TARC = \frac{\sqrt{\left|S_{11} + S_{12}\,e^{j\theta}\right|^2 + \left|S_{21} + S_{22}\,e^{j\theta}\right|^2}}{\sqrt{2}} \tag{8}$$

In Figure 13, θ is varied constantly by 30, but in each case the measured TARC follows the reflection coefficient pattern and thus maintains the resonance behavior even when the phase of the signal is changing.
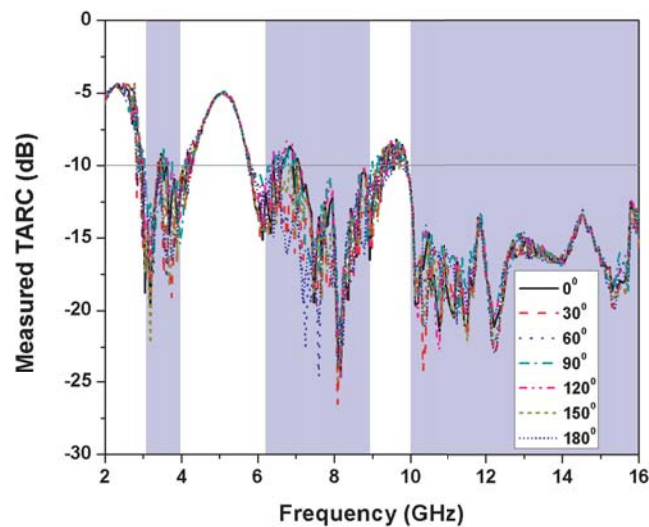

Figure 13. TARC.

5. CONCLUSION

A compact triple-band: 3.03–3.96, 6.2–8.93 & 10–16 GHz, two-port MIMO antenna with one band-notched characteristic has been presented. Two crescent ring-shaped structures have been etched on the circular radiating patch to achieve the band-notch from 3.93 to 6.2 GHz centered at 5 GHz. The radiation efficiency is as low as 20% in the band-notch which isolates the proposed MIMO antenna from the high traffic of 5.2/5.8 WLAN, 5.5 WiMAX, LMI C-band and the large capacity microwave relay trunk network ranging from 4.40 to 4.99 GHz, such as in the Indian national satellite (INSAT) system operating from 4.5 to 4.8 GHz. An isolation structure — MIDC — has been introduced to achieve a minimum measured isolation of 16 dB throughout. The isolation structure restricts the surface wave as well as the space wave propagation from one antenna to another. It also helps in achieving one center-band ranging from 6.2 to 8.93 GHz due to better impedance matching, and hence, does not cover the high traffic on the remaining 8.93–10 GHz band of the X-band in the process of covering the entire UWB. The measured results show that the gain ranges from 3.5 to 6 dBi. Our proposed antenna is useful in 3.5 GHz WiMAX, IEEE INSAT/Super Extended C-band and for the major part of X-band and Ku-band applications.

REFERENCES

1. Federal Communications Commission, "Federal Communications Commission revision of Part 15 of the commission's rules regarding ultra-wideband transmission system from 3.1 to 10.6 GHz," *ET-Docket*, 98–153, Washington, DC, USA, 2002.

2. Almalkawi, M. J. and V. K. Devabhaktuni, "Quad band-notched UWB antenna compatible with WiMAX/INSAT/lower-upper WLAN applications," *Electronics Letters*, Vol. 47, No. 19, 1062–1063, Sept. 2011.

3. Kumar, A., A. Q. Ansari, B. K. Kanaujia, and J. Kishor, "High isolation compact four-port MIMO antenna loaded with CSRR for multiband applications," *Frequenz*, 2018.

4. Iglesias, E. R., Ó. Q. Teruel, and L. I. Sánchez, "Mutual coupling reduction in patch antenna arrays by using a planar ebg structure and a multilayer dielectric substrate," *IEEE Trans. Antennas Propagat.*, Vol. 56, No. 6, 1648–1655, Jun. 2008.

5. Li, Q., A. P. Feresidis, M. Mavridou, and P. S. Hall, "Miniaturized double-layer EBG structures for broadband mutual coupling reduction between UWB monopoles," *IEEE Trans. Antennas Propagat.*, Vol. 63, No. 3, 1168–1171, Mar. 2015.

6. Habashi, A., J. Nourinia, and C. Ghobadi, "Mutual coupling reduction between very closely spaced patch antennas using low-profile Folded Split-Ring Resonators (FSRRs)," *IEEE Antennas and Wireless Propagation Letters*, Vol. 10, 862–865, Jul. 2011.

7. Suwailam, M. M. B., O. F. Siddiqui, and O. M. Ramahi, "Mutual coupling reduction between microstrip patch antennas using slotted-complementary split-ring resonators," *IEEE Antennas and Wireless Propagation Letters*, Vol. 9, 876–878, Aug. 2010.

8. Ouyang, J., F. Yang, and Z. M. Wang, "Reducing mutual coupling of closely spaced microstrip MIMO antennas for WLAN application," *IEEE Antennas and Wireless Propagation Letters*, Vol. 10, 310–313, Mar. 2011.

9. Zhang, S. and G. F. Pedersen, "Mutual coupling reduction for UWB MIMO antennas with a wideband neutralization line," *IEEE Antennas and Wireless Propagation Letters*, Vol. 15, 166–169, May 2015.

10. Gangwar, D., S. Das, and R. L. Yadava, "Reduction of mutual coupling in metamaterial based microstrip antennas: The progress in last decade," *Wireless Pers. Commun.*, Springer, Mar. 2014.

11. Tao, J. and Q. Feng, "Compact UWB band-notch MIMO antenna with embedded antenna element for improved band notch filtering," *Progress In Electromagnetics Research C*, Vol. 67, 117–125, 2016.

12. Atallah, H. A., A. B. Abdel-Rahman, K. Yoshitomi, and R. K. Pokharel, "CPW-fed UWB antenna with sharp and high rejection multiple notched bands using stub loaded meander line resonator," *International Journal of Electronics and Communications*, Vol. 83, 22–31, May 2017.

13. Mansouri, Z., F. B. Zarrabi, and A. S. Arezoomand, "Multi notch-band CPW-fed circular-disk UWB antenna using underground filter," *International Journal of Electronics Letters*, Vol. 6, No. 2, 204–213, 2018.

14. Tsai, L.-C., "A ultrawideband antenna with dual-band band-notch filters," *Microw. Opt. Technol. Lett.*, Vol. 59, 1861–1866, 2017.

15. Yin, Y. and J. S. Hong, "UWB band-notched adjustable antenna using concentric split-ring slots structure," *Frequenz*, Vol. 68, No. 9–10, 433–439, 2014.

16. Zarrabi, F. B., Z. Mansouri, N. P. Gandji, and H. Kuhestani, "Triple-notch UWB monopole antenna with fractal Koch and T-shaped stub," *AEU — International Journal of Electronics and Communications*, Vol. 70, No. 1, 64–69, 2016.

17. Chandel, R., A. K. Gautam, and K. Rambabu, "Tapered fed compact UWB MIMO-diversity antenna with dual band-notched characteristics," *IEEE Trans. Antennas Propagat.*, Vol. 66, No. 4, 1677–1684, Apr. 2018.

18. Li, W. T., Y. Q. Hei, H. Subbaraman, X. W. Shi, and R. T. Chen, "Novel printed filtenna with dual notches and good out-of-band characteristics for UWB MIMO applications," *IEEE Microwave and Wireless Components Letters*, Vol. 26, No. 10, 765–767, Oct. 2016.

19. Zhu, J., B. Feng, B. Peng, S. Li, and L. Deng, "Compact CPW UWB diversity slot antenna with dual band-notched characteristics," *Microw. Opt. Technol. Lett.*, Vol. 58, No. 4, 989–994, Feb. 2016.

20. Tang, T. C. and K. H. Lin, "An ultrawideband MIMO antenna with dual band-notched function," *IEEE Antennas and Wireless Propagation Letters*, Vol. 13, 1076–1079, 2014.

21. Lee, J. M., K. B. Kim, H. K. Ryu, and J. M. Woo, "A compact ultrawideband MIMO antenna with WLAN band-rejected operation for mobile devices," *IEEE Antennas and Wireless Propagation Letters*, Vol. 11, 990–993, 2012.

22. Gao, P., S. He, X. Wei, Z. Xu, N. Wang, and Y. Zheng, "Compact printed UWB diversity slot antenna with 5.5-GHz band-notched characteristics," *IEEE Antennas and Wireless Propagation Letters*, Vol. 13, 376–379, 2014.

23. Chacko, B. P., G. Augustin, and T. A. Denidni, "Uniplanar polarisation diversity antenna for ultrawideband systems," *IET Microwaves, Antennas & Propagation*, Vol. 7, No. 10, 851–857, Jul. 2013.

24. Kang, L., H. Li, X. Wang, and X. Shi, "Compact offset microstrip-fed MIMO antenna for band-notched UWB applications," *IEEE Antennas and Wireless Propagation Letters*, Vol. 14, 1754–1757, 2015.

25. Liu, L., S. W. Cheung, and T. I. Yuk, "Compact MIMO antenna for portable devices in UWB applications," *IEEE Trans. Antennas Propagat.*, Vol. 61, No. 8, 4257–4264, Aug. 2013.

26. Toktas, A., "G-shaped band-notched ultra-wideband MIMO antenna system for mobile terminals," *IET Microwaves, Antennas & Propagation*, Vol. 11, No. 5, 718–725, Apr. 2017.

27. Yoon, H., Y. Yoon, H. Kim, and C.-H. Lee, "Flexible ultra-wideband polarization diversity antenna with band-notch function," *IET Microwaves, Antennas & Propagation*, Vol. 5, 1463–1470, 2011.

28. Wu, W., B. Yuan, and A. Wu, "A quad-element UWB MIMO antenna with band-notch and reduced mutual coupling based on EBG structures," *Int. J. Antennas Propag.*, Vol. 2018, Feb. 2018.

29. Chandel, R. and A. K. Gautam, "Compact MIMO/diversity slot antenna for UWB applications with band-notched characteristic," *Electronics Letters*, Vol. 52, No. 5, 336–338, Mar. 2016.

30. Ellis, M. S., Z. Zhao, J. Wu, Z. Nie, and Q. Liu, "A novel miniature bandnotched Wing-Shaped monopole ultrawideband antenna," *IEEE Antennas and Wireless Propagation Letters*, Vol. 12, No. 1, 1614–1617, 2013.

31. Alley, G. D., "Interdigital capacitors and their application to lumped-element microwave integrated circuits," *IEEE Transactions on Microwave Theory and Techniques*, Vol. 18, No. 12, 1028–1033, Dec. 1970.